



Minerva Access is the Institutional Repository of The University of Melbourne

Author/s:

Kearney, MR;Porter, WP;Huey, RB

Title:

Modelling the joint effects of body size and microclimate on heat budgets and foraging opportunities of ectotherms

Date:

2021-03-01

Citation:

Kearney, M. R., Porter, W. P. & Huey, R. B. (2021). Modelling the joint effects of body size and microclimate on heat budgets and foraging opportunities of ectotherms. *Methods in Ecology and Evolution*, 12 (3), pp.458-467. <https://doi.org/10.1111/2041-210X.13528>.

Persistent Link:

<https://hdl.handle.net/11343/337968>

1
2
3
4
5
6
7
8
9
10
11
12
13
14
15
16
17
18
19
20
21
22
23
24
25
26
27
28
29
30
31

DR MICHAEL KEARNEY (Orcid ID : 0000-0002-3349-8744)

PROFESSOR RAYMOND B HUEY (Orcid ID : 0000-0002-4962-8670)

Article type : Research Article

Editor : Simone Blomberg

Modeling the joint effects of body size and microclimate on heat budgets and foraging opportunities of ectotherms

Michael R. Kearney¹, Warren P. Porter² and Raymond B. Huey⁵

¹School of BioSciences, The University of Melbourne, Melbourne, Victoria 3010 Australia

²Department of Zoology, University of Wisconsin, 250 North Mills Street, Madison, WI 53706 USA

³Department of Biology, University of Washington, Seattle, WA 98195 USA

Corresponding author: Michael R. Kearney, BioSciences 4, School of BioSciences, The University of Melbourne, Melbourne, Victoria 3010 Australia, email: m.kearney@unimelb.edu.au

Running headline: Size and microclimate constraints on foraging ectotherms

Abstract

1. Body size affects the body temperature of an ectotherm by altering both heating rates and the microclimate experienced. These joint effects are rarely considered in analyses of climatic constraints on ectotherms but nonetheless influence body temperatures and thus activity periods and foraging opportunities.
2. Here we develop and test transient heat-budget models that use height-specific microclimatic forcing to compute the dynamics of size-dependent body temperatures

This is the author manuscript accepted for publication and has undergone full peer review but has not been through the copyediting, typesetting, pagination and proofreading process, which may lead to differences between this version and the [Version of Record](#). Please cite this article as [doi: 10.1111/2041-210X.13528](https://doi.org/10.1111/2041-210X.13528)

This article is protected by copyright. All rights reserved

32 of ectotherms in sun and in shade. We incorporate a model of behavioural
 33 thermoregulation and use it to compute potential body temperatures and then to map
 34 these to ecologically relevant indices, including foraging opportunities and thermal
 35 constraints. To illustrate potential applications, we combine a microclimate model
 36 driven by a global climate database with the transient behavioural algorithm
 37 developed for lizards to explore how body size (10 g and 1000 g) and size-specific
 38 microclimate (at natural heights of 1 and 7.5 cm, respectively) interactively influence
 39 body temperatures and ecological indices at a warm, arid location in Australia in both
 40 spring and summer. To explore microclimatic effects, we contrast temperatures and
 41 indices for animals positioned at their natural versus reciprocal heights above the
 42 ground.

- 43 3. Our simulations show that the behavioural and ecological consequences of size can be
 44 strongly biased when joint effects of body size and size-imposed microclimate are
 45 ignored. For example, the two body sizes did not differ in total foraging time when
 46 compared at their natural heights, but did differ if compared at the same height, the
 47 direction of this difference reversing with the height at which they were compared.
 48 We show how computed foraging times can be translated to potential foraging radii
 49 from a central place (burrow or shade-providing bush), thereby illustrating how body
 50 size can be physiologically translated into habitat connectivity as a function of
 51 different shade configurations, e.g. as modified by fire regimes or shrub dieback.
- 52 4. All functions are now integrated into the biophysical modeling R package
 53 NicheMapR and as a Shiny app, which should provide new insights and avenues for
 54 investigation into functional interactions between body size and habitat structure for
 55 ectotherms.

56 **KEYWORDS**

57 scaling, heat exchange, microclimate, terrestrial ectotherm, foraging, thermoregulation,
 58 shade, fire

59 **Introduction**

60 Evaluating when, where, and for how long an ectotherm can safely forage in the open
 61 without overheating is a fundamental question in physiological and behavioural ecology. The
 62 empirical significance of this problem has been long recognized. For instance, Norris (1967)
 63 noted that hatchling *Uta stansburiana* lizards that are “*placed between bushes seven or eight*
 64 *feet apart at midday often will die before reaching shelter.*” Similarly, Tinkle (1967) wrote
 65 that “*Less than one minute on the hot sand on a clear day was required to raise body*

66 *temperature to a critical point*' for adult *Uta stansburiana*. The configuration of shade in a
67 habitat directly affects the thermoregulatory responses of ectotherms (Sears et al., 2016) and
68 climate warming may alter activity budgets by increasing shade requirements (Sinervo et al.,
69 2010; Michael R. Kearney, 2013). Shade configuration is being significantly altered on a
70 global scale through habitat destruction and changed fire regimes, increasing the practical
71 relevance of understanding the resulting thermal constraints on foraging in ectotherms such
72 as lizards.

73 Biophysical (heat-transfer) models can quantify these dynamics, and they do so by
74 determining how microenvironments experienced by an organism affect its body temperature
75 (T_b) and in turn its potential movement and foraging options. Most biophysical models are
76 steady-state and may be inappropriate for analyzing movement options and constraints for
77 two reasons:

- 78 (1) They assume that T_b equilibrates instantly with environmental conditions
79 (Buckley, 2008; Michael R. Kearney, Shine, & Porter, 2009; Sunday et al., 2014;
80 Pinsky, Eikeset, McCauley, Payne, & Sunday, 2019; but see Christian, Tracy, &
81 Tracy, 2006; Rubalcaba, Gouveia, & Olalla-Tárraga, 2019). However, T_b will not
82 equilibrate instantly because all organisms have thermal inertia, especially as size
83 increases over 100 g (Spotila, Soule, & Gates, 1972; Willmer & Unwin, 1981;
84 Stevenson, 1985; Seebacher & Shine, 2004). We refer to this size-dependent lag
85 as the 'Newtonian effect,' in reference to Newton's law of cooling (Figure 1a).
86 (2) Moreover, small and large organisms necessarily experience different
87 microenvironments, simply because their bodies are at different heights above
88 ground (Muth, 1977). At midday on the ground in the open sun, for example, a
89 large animal will be in a cooler microenvironment than will a small animal simply
90 because air temperature declines and wind speed increases with height above
91 ground (Geiger, 1950). Thus, the animal's convective microenvironment is body
92 size-dependent; we refer to this as the 'Geigerian' effect (Figure 1b) with
93 reference to Geiger's (1950) classic treatise on microclimates.

94 We know of no biophysical modelling studies that jointly consider the 'Newtonian' and
95 'Geigerian' effects when evaluating the effects of size and microclimate on ectotherms.
96 However, the importance of the Geiger effect is illustrated by reconsidering a classical result
97 in biophysical ecology (Willmer & Unwin, 1981; Stevenson, 1985), namely that large
98 ectotherms in sun have higher steady-state T_b than do small ones because large animals have
99 relatively thick boundary layers and thus are less tightly coupled to the convective

100 environment than are small animals (Figure 1). The empirical (Willmer & Unwin, 1981)
101 demonstration of this size effect was, however, based on insects suspended at a fixed height
102 above ground (thus in same microclimates, P. Willmer, personal communication). Similarly
103 the theoretical model also assumed that microclimate was independent of size (Stevenson,
104 1985). Nevertheless, if animals are heated at their normal height above ground, the classical
105 size effect can be reversed, such that small ectotherms can have the higher steady-state T_b
106 (justified below).

107
108 Here we develop a generic, transient heat-budget model for the R programming
109 environment. The model is suitable for small to moderate-sized organisms and captures heat-
110 flow via radiation and convection for different geometries. Using lizard-sized ectotherms as
111 examples, we illustrate how this heat budget model can be forced with size-specific modelled
112 microclimate inputs (Michael R. Kearney, Isaac, & Porter, 2014; Michael R. Kearney &
113 Porter, 2017). We also develop an explicit model of behavioural thermoregulation that is
114 incorporated into the Ordinary Differential Equation (ODE) solver routines such that, when
115 T_b crosses a set-point threshold, an appropriate behavioural shift (e.g., thermoregulatory
116 shuttling between sun and shade) is triggered. We then use the behavioural model to predict
117 potential body temperatures of small (10 g) and large (1000 g) animals in sun or in shade at
118 different times (day, season) in a hot, arid location.

119 Model derived estimates of T_b over time are relevant to ecology in several ways.
120 First, because T_b affects an animal's physiological capacities, T_b can be mapped onto a
121 performance or fitness index (Huey & Slatkin, 1976; Tracy & Christian, 1986; Vasseur et al.,
122 2014). Second, the animal's current T_b and environment will also influence the animal's
123 immediate behavioural options and constraints, such as how far it can safely forage away
124 from shade without overheating or how soon it must shuttle to shade. Here T_b is mapped onto
125 ecological or behavioural indices, a concept that traces to three papers published in 1967
126 (Janzen, 1967; Norris, 1967; Tinkle, 1967) and that anticipates the thermal safety margin
127 (Heatwole, 1970; Deutsch et al., 2008). Third, the behavioural and movement options (above)
128 can be overlaid on a habitat map with scattered patches of shade, and thus can measure the
129 thermal quality and connectivity of the habitat from an ectotherm's perspective.

130 We show that values of all these indices can differ strikingly depending on whether a
131 Newtonian vs. Geigerian perspective is adopted. We discuss the modelling framework in the
132 contexts of interpreting thermoregulatory behaviour and of understanding shade-related
133 habitat modifications, such as fire, land-clearing, or plant dieback.

134

135 **Methods**136 Transient heat budget models

137 The transient heat budget models presented here are expansions on Porter et al.
 138 (1973), which developed equations based on an analogy of electrical circuits involving
 139 capacitors and resistors. A key decision is whether to assume that the body is at uniform
 140 temperature in a given moment and so can be considered as ‘one lump’, or whether the body
 141 must be broken into ‘two lumps’ with an inner core and outer shell, each of which may be at
 142 different temperatures in a given moment. One lump is adequate for small ectotherms but not
 143 for large ones ($> \sim 1$ kg), although exactly how large depends on the environmental context
 144 and specific organismal traits (Porter et al., 1973). In Supporting Information Appendix S1,
 145 we derive equations for solving one lump and two lump models.

146 In summary, for the ‘one lump’ scenario for an ellipsoid-shaped object with
 147 convective and radiative exchange without metabolic heat generation, the rate of change in
 148 body temperature is:

$$149 \frac{dT_c}{dt} = \frac{Q_{sol}}{C} + \frac{T_a}{CR_{conv}} + \frac{T_{rad}}{CR_{rad}} - \frac{T_c}{C} \left(\frac{1}{R_{rad}} + \frac{1}{R_{conv}} \right) \quad (\text{eq. 1})$$

$$150 = \frac{1}{C} [Q_{sol} + A(h_{conv}T_a + h_{rad}T_{rad})] - \frac{A(h_{conv} + h_{rad})}{C} T_c \quad (\text{eq. 2})$$

151

152 where T_c , T_a , and T_{rad} are core, air and radiant environmental temperature, respectively ($^{\circ}\text{C}$),
 153 $C = \rho V c_p$ is heat capacity (Joules, where ρ is density kg/m^3 , V is volume m^3 and c_p is specific
 154 heat capacity J kg^{-1}), Q_{sol} is solar radiation absorbed (W), h_{conv} is the convective heat transfer
 155 coefficient ($\text{Watts m}^{-2} \text{ } ^{\circ}\text{C}^{-1}$), $h_{rad} = 4\epsilon\sigma T_{ave}^3$ ($\text{Watts m}^{-2} \text{ K}^{-1}$) is a Taylor-series approximation
 156 of the radiative heat transfer coefficient where ϵ is emissivity (-), σ is the Stefan-Boltzmann
 157 constant ($5.67 \times 10^{-8} \text{ Watts m}^{-2} \text{ K}^{-4}$), and T_{ave} is the average of the organism’s surface
 158 temperature T_s and radiant environmental temperature T_{rad} (K). The one lump model
 159 assumes that $T_s = T_c$. In a constant environment, Eq. 2 can be solved analytically for any
 160 time t , specifically $T_c = (T_{c,i} - T_{c,f})e^{-\frac{t}{\tau}} + T_{c,f}$ (see Appendix S1) where the time constant τ
 161 $= \frac{C}{A(h_{conv} + h_{rad})}$, $T_{c,i}$ is the initial temperature, and $T_{c,f} = \frac{Q_{sol} + A(h_{conv}T_a + h_{rad}T_{rad})}{A(h_{conv} + h_{rad})}$ is the final
 162 temperature, with $T_s = T_c$ for the infrared radiation calculations.

163

164 Implementation in the NicheMapR package

165 The analytical function for the ‘one lump’ model described above is implemented as
166 function **onelump** in the NicheMapR package, for example:

```
167 library(deSolve) # load the deSolve package  
168 library(NicheMapR) # load the NicheMapR package  
169 t <- seq(1, 3600 * 2, 60) # times (in seconds) to report back  
170 values  
171 Ww_g <- 10 # body wet weight, g  
172 Tc_init <- 27.4 # initial body temperature, °C  
173 geom <- 2 # shape (2 = ellipsoid)  
174 Tair <- 38.4 # air temperature, °C  
175 Trad <- Tair # radiant temperature, °C  
176 vel <- 0.57 # wind speed, m/s  
177 Qsol <- 811 # horizontal plane solar radiation, W/m2  
178 Zen <- 51 # zenith angle of sun, degrees  
179 alpha <- 0.85 # solar absorptivity, -  
180 Tb <- onelump(t = t, alpha = alpha, Tc_init = Tc_init, Ww_g =  
181 Ww_g, geom = geom, Tair = Tair, Trad = Trad, vel = vel, Qsol =  
182 Qsol, Zen = Zen)
```

183
184 Results from the code above are included in Figure 2, which shows computed heating
185 rates and steady-state T_b s of 10 g and 1000 g ectotherms over 2 hours starting at midday in
186 mid-September at Newhaven Wildlife Sanctuary in central Australia. Figure 2a assumes a
187 Newtonian perspective, with both animals suspended in air at 7.5 cm, which is the natural
188 height of the large ectotherm. The T_b of the 10 g ectotherm equilibrates faster (~ 10 vs. ~
189 100+ minutes) but at a lower temperature than that of the 1000 g ectotherm (~ 41° vs. ~
190 45°C), as expected (Stevenson, 1985). Figure 2b assumes a Geigerian perspective, with the
191 small and large ectotherms positioned at their natural heights (1 vs. 7.5 cm, respectively).
192 Here the T_b of the small ectotherm still equilibrates relatively quickly (~ 15 min) but now at a
193 higher T_b than that of the large ectotherm (~ 47° vs. 45°C). This happens because the small
194 ectotherm is lower in the boundary layer of the ground and thus exposed to lower wind
195 speeds and higher air temperatures (i.e., Geiger counts!).

196 For the ‘one lump’ model under changing environmental conditions, and for the ‘two
197 lump’ model in general, solutions must be obtained numerically using an ordinary differential
198 equation solver. The functions **onelump_var** and **twolump** of the NicheMapR package

199 use the R package ‘deSolve’ (Soetaert, Petzoldt, & Setzer, 2010), with the forcing variables
200 being interpolated between time steps by using the base R function `approxfun`.

201 The required forcing data can be obtained either from empirical microclimate
202 measurements or from outputs of the microclimate model of NicheMapR (Michael R.
203 Kearney & Porter, 2017). Applications using the microclimate model are illustrated in the
204 help documents for the `one_lump_var` and `two_lump` functions. The one lump algorithm is
205 incorporated into the `ectotherm` function of NicheMapR (Michael R. Kearney & Porter,
206 2019) and the transient case can be invoked by setting the option ‘transient’ to value 1. The
207 algorithm is then solved using the DOPRI5 numerical integrator (Hairer, Norsett, & Wanner,
208 1993) (note, the `ectotherm` model implementation of the transient equations does not yet
209 incorporate thermoregulatory behaviour).

210

211 Model tests

212 We tested the ability of the `one_lump` and `two_lump` functions to capture observed
213 daily temperature variation in two sets of inanimate objects; (1) hollow copper and water-
214 filled PVC pipes of different lengths, diameters and solar absorptivities, and (2) fruits of
215 various sizes and colors (peaches, cantaloupe and watermelon). Full details of the methods
216 and test outcomes are provided in Supporting Information (Appendices S2 & S3). Also, we
217 compared model predictions against observations of two lizards, a military dragon
218 *Ctenophorus isolepis* (~10 g) and a sand goanna *Varanus gouldi* (~1 kg) [see Supporting
219 Information for methods and results].

220

221 Behavioural thermoregulatory algorithm

222 We considered a diurnally-active animal that spends the full 24-h day on the ground
223 surface (i.e., does not climb or burrow; however, burrowing could be simulated by making
224 radiant and air temperatures equal to soil temperature at a specified depth). We then
225 developed a modelling scheme that incorporates transient heat budget functions and captures
226 key thermoregulatory behaviours, including postural adjustments and shuttling between sun
227 and shade through the course of a day. Behavioural shifts are initiated when T_b crosses a
228 specified temperature threshold and triggers an exit from the ODE solver so that particular
229 behaviours can be invoked. These user-adjustable thresholds are collected in the function
230 `trans_behav` of NicheMapR (which could be modified for other motivations to move
231 such as hunger, moisture). The function takes as input forcing data the ‘metout’, ‘shadmet’,

232 ‘soil’ and ‘shadsoil’ outputs of the NicheMapR microclimate model, and then estimates
233 hourly local air temperature and wind speed, surface and sky temperature, solar radiation and
234 zenith angle, for sun and shade.

235 Specifically, the animal starts in maximum ‘shade’ at hour 0 (nighttime). After
236 sunrise, the animal remains in shade; and its T_b gradually warms as ambient temperature
237 rises. Once T_b in shade reaches the animal’s minimum basking temperature (T_{b,min_bask}), the
238 animal moves into sun (“emerge” event) and begins basking (body oriented perpendicular to
239 the sun’s rays). It remains basking until its T_b reaches the minimum activity temperature
240 ($T_{b,min_activity}$), when it begins foraging in the open (“forage” event) in a posture averaged
241 between perpendicular and parallel to the sun’s rays. It continues foraging in the sun until its
242 T_b reaches the animal’s maximum acceptable body temperature $T_{b,max_activity}$, whereupon the
243 animal retreats to shade (“shuttle” event). Once its T_b cools to at or near $T_{b,min_activity}$, or to the
244 shaded air temperature (if this is above $T_{b,min_activity}$), the animal moves back to the sun and
245 resumes foraging (new “forage” event); and so on throughout the morning. If T_b in the shade
246 rises above $T_{b,max_activity}$ the animal simply remains in the shade and tolerates the conditions.
247 Once temperatures cool in the afternoon, it resumes shuttling until T_b drops below T_{b,min_bask}
248 or until the sun is down: in either case, the animal then ceases activity and retreats to full
249 shade (“retreat” event) for the night.

250 These four events – “emerge”, “forage”, “shuttle” and “retreat” – are passed to the
251 ODE solver and conditionally impose a value of zero on the solution to trigger an exit from
252 the solver so that new environmental conditions can be selected. The “forage” event required
253 special care in how it referred to shaded air temperature, $T_{air,shd}$. In the case of an animal
254 cooling in an environment where $T_{air,shd}$ was greater than $T_{b,min_activity}$ (as might occur in
255 midday heat), the threshold value to emerge needed to be set somewhat warmer than $T_{air,shd}$:
256 otherwise, the lag-effect of large body mass during afternoon cooling prevented re-emergence
257 in some cases. For our analyses, a 1°C offset sufficed. In addition, when $T_{air,shd}$ was
258 approaching $T_{b,max_activity}$ (as might occur on hot days), animals would emerge but engage in
259 unrealistically short foraging bouts. Thus, a value somewhat less than $T_{b,max_activity}$ was used to
260 trigger foraging in this circumstance (for our analyses, a 2 °C offset sufficed). On very hot
261 days, even T_b in shade at midday may exceed $T_{b,max_activity}$; in this case the animal remains in
262 shade and potentially may even be forced to experience temperatures above CT_{max} . [Note:
263 the `trans_behav` code can be adapted to allow retreat to a burrow or to an elevated perch, if
264 appropriate.]

265

266 Ecological Indices

267 The above heat-transfer and behavioural models produce a time series of potential T_b
 268 of animals moving about an open habitat and shuttling to shade. We converted these to
 269 ecological indices that include times or distances, which are interconvertible [assuming
 270 movement speed is independent of T_b within the range of activity T_b]:

271 (1) *Cumulative hours (or total distance covered) of foraging* (i.e., time when T_b is
 272 within the foraging range in the open) during a given day indexes a temporal (or spatial)
 273 aspect of a habitat's thermal suitability.

274 (2) *Number of shuttling bouts per day* indexes how frequently the organism is forced
 275 to retreat to shade and gives an indication of the costs of thermoregulatory behaviours such as
 276 locomotion costs and time potentially lost from other activities (foraging, courtship), and
 277 increased conspicuousness to predators (Huey & Slatkin, 1976).

278 (3) *Duration (distance) of the longest foraging bout* during the day measures the
 279 duration (distance) of a single best foraging opportunity as well as the maximum safety factor
 280 (time to forage and to return to shade without T_b exceeding $T_{b,max_foraging}$). The maximum
 281 duration (distance) is $\frac{1}{2}$ that of the maximal time (distance) time of a single foraging bout.

282 (4) *Cumulative hours of restriction to shade* estimates the total time per day when T_b
 283 in open is too hot for foraging (i.e., above $T_{b,max_activity}$), and thus indexes environmental
 284 restrictions on foraging in the open (Sinervo et al., 2010).

285 In addition, we show how foraging radii can be mapped onto shade configurations in
 286 different habitats to determine spatial and temporal patterns of connectivity (Sears et al.,
 287 2016).

288

289 Simulation studies

290 We simulated a small (10 g) and large (1000 g) lizard at a hot site in central Australia
 291 (Newhaven Wildlife Sanctuary, 131.170° longitude, -22.724° latitude, 559 m). The mid-point
 292 of the body of the small and the large lizard was assumed to be 1 cm or 7.5 cm above the
 293 ground, respectively. In the absence of scaling data on field foraging speeds in nature, we
 294 assumed that the small and large lizards forage at speeds of 0.3 and 0.75 km/h, respectively,
 295 to demonstrate the approach. We used the `micro_global` function of NicheMapR to
 296 compute hourly microclimates for an average day in spring (September) and in summer
 297 (January). We assumed that both lizards would initiate basking at a T_b of 18 °C and forage
 298 between 33 °C and 43 °C (Pianka, 1971; King, 1980).

299

300 **Results**

301 The hourly simulation outputs for the two lizards at their natural and reciprocal
302 heights in two seasons are presented in Figure 3. We begin by looking at the Newtonian
303 effect on small and then on large animals in September (Austral spring) and again in January
304 (Austral summer) at a site in central Australia. Then we compare Geigerian effects of size of
305 lizards at their natural heights. The specific results are, of course, contingent on the explicit
306 assumptions (e.g., sizes, event thresholds), but nonetheless serve as heuristic examples of
307 why size-specific microclimates matter. Finally, we compare the model's predictions to the
308 behaviours of small and large lizards foraging contemporaneously at the study site in
309 October.

310

311 *Cumulative hours of foraging and number of shuttling bouts*

312 **September** (spring): If small and large lizards experience identical microclimates,
313 the small animal should warm faster and thus have an earlier onset of foraging (Stevenson,
314 1985). Indeed, when both lizards are compared at a height of 7.5 cm (Newtonian
315 comparison), the small lizard does heat faster and begins foraging earlier (~ 0945 vs. ~ 1020
316 h, Figures 2b & 2c). Nevertheless, the large lizard has a longer (cumulative) activity period in
317 sun than does the small lizard (5.9 vs. 5.1 h, Figure 4a). Greater activity of the large lizard in
318 this cool season reflects in part its hotter maximum potential T_b in the open, $T_{b,open}$, at midday
319 (44.0 vs. 40.7 °C), which elevates its heating rate (Figures 2b & 2c). At this height in this
320 cool month, neither lizard needs to shuttle to shade.

321 When the small lizard is at its natural height (1 cm), it still has the earlier onset of
322 activity (0914 vs 0941 h, Figure 2a & d) but now has a longer activity period than would the
323 large lizard lowered to that same height (6.2 vs. 5.1 h, Figure 4a). At this low height both
324 sizes need to shuttle, but the large lizard's higher maximum $T_{b,open}$ (50.1 vs. 46.6 °C, Figures
325 2a & d) forces it to shuttle over a longer time window and to lose more time in the shade
326 attempting to cool. When both lizards are at their natural heights, neither must shuttle; and
327 both lizards have similar activity times (6.0 vs. 5.9 h, Figures 2a & 2b).

328

329 **January** (summer). When compared at 7.5 cm, the large lizard has a slightly shorter
330 activity period than does the small lizard (5.5 vs 5.9 h, Figure 4a) but shuttles many fewer
331 times (10 vs 50/day, Figure 4b & Figures 2f vs. 2g). Overheating is a risk for both the small
332 and the large lizard, as their maximum T_e (50.3 vs. 53.6 °C, respectively) are higher than their
333 shared CT_{max} (48 °C). When compared at 1 cm, the small lizard has the longer activity period

334 (4.9 vs. 4.6 h, Fig. 4a) but again must shuttle to shade much more frequently than does the
335 large lizard (52 vs. 10/day, Figure 4b & Figures 2e vs. 2h). When both are at their natural
336 height, the larger lizard has the longer activity time (5.5 vs. 4.9 h, Figure 4a), and the small
337 lizard still shuttles much more frequently (52 vs. 10/day, Figure 4b & Figures 2e vs. 2f).

338

339 *Distance (and duration) of the single longest foraging bout*

340 **September.** When compared at 7.5 cm, the large lizard has a slightly longer
341 maximum foraging bout (5.9 vs. 5.1 h, Figure S1; identical to the total foraging time reported
342 above because no shuttling occurs). The small lizard is unable to move nearly as far from
343 shade as can the large lizard (0.7 km vs. 2.2 km, Figure 4c), reflecting its lower speed and
344 reduced thermal inertia. When the small lizard is at 1 cm, its natural height, it has a slightly
345 longer maximal foraging bout than a large lizard at that height (2.5 h vs. 2.5 h, Figure S1).
346 However, if the large lizard is at its natural height, its maximum foraging bout has increased
347 substantially and has become much longer than that of the small lizard at its natural height
348 (5.9 vs. 2.5 h, Figure S1), simply because the small lizard must shuttle frequently whereas the
349 large lizard need not. Furthermore, the large lizard can always move substantially further
350 from shade due to its greater assumed movement speed and thermal inertia (Fig. 4c).

351

352 **January.** When both are compared at 7.5 cm, the small lizard has a slightly shorter
353 foraging bout than the large lizard (2.1 vs. 2.3 h, Figure S1) but, again, the small lizard
354 cannot move nearly as far from shade as the large lizard (0.3 vs. 0.85 km, Fig. 4c) due to its
355 lower movement speed and lower thermal inertia. Qualitatively similar patterns (1.7 vs. 1.7 h,
356 0.25 vs 0.65 km) hold if both are compared at 1 cm (Figures S2 and 4c, respectively). When
357 compared at their natural heights, the small lizard has a shorter maximum foraging bout (1.7
358 vs 2.4 h, Fig. S1) and a much shorter maximum foraging radius away from shade (0.25 vs.
359 0.85 km, Figure 4c).

360

361 *Cumulative hours of restriction to shade*

362 **September.** When compared at 7.5 cm in this cool month, neither lizard needs to
363 retreat to shade (Figures 2b & 2c, Figure 4d). At 1 cm, however, the small and large lizards
364 need to cool in shade for 30 and 89 min per day, respectively (Figure 4d). When compared at
365 their natural height, only the small lizard needs access to shade (30 vs. 0 min, Figure 4d).

366 **January.** When compared at 7.5 cm or at 1 cm, both lizards need access to shade for
367 considerable periods (small = 224 vs. 288 min; large = 326 vs. 383 min, Figure 4d). When

368 compared at their natural height, the small lizard is restricted to shade for slightly longer than
369 the large lizard (326 vs. 288 min, Figure 4d).

370

371 *Translation to space access*

372 By mapping the maximum foraging radii computed above onto particular habitat
373 configurations, the degree of habitat connectivity can be assessed from a physiological
374 perspective. Figure 5 illustrates this by plotting radii from 50 randomly distributed shade
375 points (e.g. bushes, burrows) across a 10 x 10 km landscape, for each of season, size and
376 microclimate scenarios considered in Figures 2-4. In spring, this arbitrary habitat
377 configuration of highly dispersed shade (~ 2 or 3 km between shade patches) would enforce
378 'central-place' foraging for the small lizard at its natural height but would be almost fully
379 connected for the large lizard at its natural height but less so at 1 cm (Figures 5a & 5b). The
380 physiological connectivity of this habitat for the two lizards at their reciprocal heights in
381 spring would be very similar and low (Figures 5c & 5d). The situation is more extreme in the
382 summer (Figs. 5e-h) when even the large lizard at its natural height would have extremely
383 restricted movement.

384

385 **Discussion**

386 Attempts to model behavioural thermoregulation have used a variety of approaches,
387 from simplified steady-state analyses that can bound the physical possibilities (Porter et al.,
388 1973; Michael R. Kearney et al., 2009), to detailed individual-based models that are explicit
389 about environmental heterogeneity and movement patterns (Sears & Angilletta, 2015; Sears
390 et al., 2016) and variants in between (Rubalcaba et al., 2019). As always, the appropriate tool
391 depends on the question being asked. The tool we developed here provides a simple means to
392 assess how body size, height above ground, and habitat quality interact from the perspective
393 of a given thermal physiology. Our analysis is unique in considering jointly the biophysical
394 and microclimatic consequences of body size, what we have called the 'Newtonian' and
395 'Geigerian' effects, respectively.

396

397 *Ecologically relevant indices and the Geiger effect*

398 The ecological indices we developed capture aspects of the costs and benefits of
399 behavioural regulation regarding foraging time, shuttling frequency, foraging duration and
400 radius, and the time spent inactive in the shade. Our analyses are designed and interpreted for
401 a species that forages predominantly in open (sunny) environments, but the same indices and

402 analyses can developed for a species that bask in sun but forages in the shade inside a forest.
403 (e.g., *Ameiva*, van Berkum, Huey, & Adams, 1986).

404 Most significantly, the interpretation of all our analyses changes – qualitatively or
405 quantitatively – depending on whether different sized lizards are at their natural heights or at
406 the same height (Figure 4). This height effect is most dramatic for total activity time (Figure
407 4a) where, in spring, we would have concluded that big lizards had the greater activity time if
408 both were at 7.5 cm, whereas that small lizards would have had greater activity time if both
409 were at 1 cm. But if both are at their natural heights, they have nearly identical activity times.
410 For this index in summer, we would have concluded that smaller lizards had greater activity
411 time at either height but in fact, at their natural heights, the larger lizard has greater activity
412 time. For all other metrics there are significant qualitative or quantitative changes of
413 interpretation if both the Geigerian and Newtonian consequences of body size are ignored
414 (Fig. 4). Ultimately, a more general analysis is required to explore how size, microclimate,
415 and thermoregulatory parameters interactively affect ecological consequences, but the simple
416 cases here are sufficient to indicate that Geigerian effects are potent and must not be ignored
417 when studying the thermal consequences of body size.

418

419 ***Translation to habitat quality***

420 We use access to shade as an indicator of the connectedness of the landscape, at least
421 in hot environments (Figure 5). For landscapes with limited shade, a longer foraging distance
422 enhances connectivity from a lizard’s perspective. Consequently, a given landscape is in
423 effect more connected for a large than for a small lizard: large lizards can cover more ground
424 because of their relatively faster walking speeds, greater thermal inertia, and cooler
425 microenvironments. As a result, large ectotherms can exploit more of warm habitats than can
426 a small ectotherm, which cannot venture far from shade. Very likely, this constraint will
427 cause small ectotherms to deplete the food in the vicinity of its shade retreat (though of
428 course its metabolic needs are less than that of a large ectotherm), and reduced food
429 consumption will exacerbate sensitivity to high temperature (Brett, 1971; Huey &
430 Kingsolver, 2019). On the other hand, the greater ranging capacity of a large ectotherm may
431 increase its spatial overlap with other large individuals, leading to resource depletion (Jetz,
432 Carbone, Fulford, & Brown, 2004). The typically positive scaling of territory (home-range)
433 size with body size has traditionally been explained in energetic terms (McNab, 1963;
434 Schoener, 1968). Our simulations suggest that in warm habitats, the scaling of home-range
435 size may also reflect size-dependent thermal considerations.

436
437
438
439
440
441
442
443
444
445
446
447
448
449
450
451
452
453
454
455
456
457
458
459
460
461
462
463
464
465
466
467
468
469

Comparison with real lizards

Comparison of our model results with detailed observations of the behaviour of two field-active lizards (Supporting Information) provides a small-scale reality check as well as an example of the value in having a model of physical expectation when interpreting such data. The behaviour of the two lizards was consistent with the model in that the large lizard was able to forage during the period when the small lizard was confined to a shade patch (Figure S4). But having the model predictions led us to new ideas about the lizard's behaviour. For instance, during the periods where the model indicated that the military dragon could forage in the open only by frequent shuttling, the military dragon neither shuttled nor retreated to a burrow. Rather, it waited in the shade at as low a temperature as it could achieve and dashed out only to capture passing prey items. Starting from a low temperature on these foraging bouts of course acts to maximise the time available to chase down prey observed beyond their shade patch. The strategy is obvious in retrospect, but apparently only after comparing predicted and observed behaviour. Such behaviour is probably widespread; one of us (WPP) has observed similar behaviour in the desert iguana *Dipsosaurus dorsalis* under extremely hot conditions.

Model applications to environmental change

Habitat destruction, plant dieback from climate stress, storms, and fire all decrease the amount of shade in a habitat. In some cases, decreases are small and transient, but other cases (as in recent fires in Australia) shade is essentially eliminated for years or perhaps decades. Decreased shade will reduce habitat connectivity as well as 'social' connectivity for ectotherms, especially for small ones. The model we have presented can quantify how reductions in the size and number of shade patches – whatever the cause – can constrain movement options of ectotherms of different sizes.

The Shiny app we have created to run the simulations via a graphical user interface (Supporting Information Appendix S4, http://bioforecasts.science.unimelb.edu.au/ectotherm_transient/) includes tools for visualising the results in comparison with satellite imagery and will facilitate applied use of the approach in managing and accessing thermal aspects of habitat connectivity.

ACKNOWLEDGEMENTS

This article is protected by copyright. All rights reserved

470 We thank the Australian Wildlife Conservancy and Danae Moore and Josef Schofield
471 for permission and support with the lizard field work on Newhaven Wildlife Sanctuary, and
472 the Walpiri Rangers (Anslem, Christine, Alice, Nelson, Benedict), Elia Pirtle, Adam Stow,
473 James Maino and Steve Comber for invaluable assistance in goanna (wardapi) catching.
474 Lizard work was done under The University of Melbourne animal ethics permit AEC1413371
475 and supported by an Australia and Pacific Science Fund grant APSF1305 to M.R.K., an
476 Australian Research Council Discovery Grant DP140101240 to M.R.K., and National
477 Science Foundation grant IOS 1038016 to R.B.H.

478

479 **AUTHORS' CONTRIBUTIONS**

480 M.R.K., R.B.H and W.P.P designed the study; W.P.P. and M.R.K. developed the models;
481 M.R.K. collected the empirical data, M.R.K. and R.H.B. performed the simulations and
482 analysed the data, M.R.K. and R.B.H, wrote the first draft of the paper with contributions
483 from W.P.P. All authors contributed critically to the drafts and gave final approval for
484 publication.

485

486 **DATA AVAILABILITY STATEMENT**

487 All data used in the tests of the model provided in the Supporting Information are available
488 via Zenodo (Kearney, 2020a). The NicheMapR release relevant to this paper (v3.0.0) is also
489 available via Zenodo (Kearney, 2020b).

490

491 **ORCID**

492 *Michael R. Kearney* <https://orcid.org/0000-0002-3349-8744>

493 *Warren P. Porter* <https://orcid.org/0000-0003-0156-4222>

494 *Raymond B. Huey* <https://orcid.org/0000-0002-4962-8670>

495

496 **REFERENCES**

- 497 Brett, J. R. (1971). Energetic responses of salmon to temperature. A study of some thermal
498 relations in the physiology and freshwater ecology of sockeye salmon (*Oncorhynchus*
499 *nerka*). *American Zoologist*, 11(1), 99–113.
- 500 Buckley, L. B. (2008). Linking traits to energetics and population dynamics to predict lizard
501 ranges in changing environments. *The American Naturalist*, 171(1), E1–E19.
- 502 Christian, K. A., Tracy, C. R., & Tracy, C. R. (2006). Evaluating Thermoregulation in
503 Reptiles: An Appropriate Null Model. *The American Naturalist*, 168(3), 421–430.

- 504 doi:10.1086/506528
- 505 Deutsch, C. A., Tewksbury, J. J., Huey, R. B., Sheldon, K. S., Ghalambor, C. K., Haak, D.
506 C., & Martin, P. R. (2008). Impacts of climate warming on terrestrial ectotherms
507 across latitude. *Proceedings of the National Academy of Sciences*, *105*(18), 6668–
508 6672. doi:10.1073/pnas.0709472105
- 509 Geiger, R. (1950). *The Climate Near the Ground*. Cambridge, Mass.: Harvard University
510 Press.
- 511 Hairer, E., Norsett, S. P., & Wanner, G. (1993). *Solving ordinary differential equations I.*
512 *Nonstiff problems*. Berlin Heidelberg: Springer-Verlag.
- 513 Heatwole, H. (1970). Thermal ecology of the desert dragon, *Amphibolurus inermis*.
514 *Ecological Monographs*, *40*(4), 425–457.
- 515 Huey, R. B., & Kingsolver, J. G. (2019). Climate Warming, Resource Availability, and the
516 Metabolic Meltdown of Ectotherms. *The American Naturalist*, *194*(6), E140–E150.
517 doi:10.1086/705679
- 518 Huey, R. B., & Slatkin, M. (1976). Cost and benefits of lizard thermoregulation. *The*
519 *Quarterly Review of Biology*, *51*(3), 363–384.
- 520 Janzen, D. H. (1967). Why mountain passes are higher in the tropics. *American Naturalist*,
521 *101*(919), 233–249.
- 522 Jetz, W., Carbone, C., Fulford, J., & Brown, J. H. (2004). The Scaling of Animal Space Use.
523 *Science*, *306*(5694), 266–268. doi:10.1126/science.1102138
- 524 Kearney, Michael R. (2013). Activity restriction and the mechanistic basis for extinctions
525 under climate warming. *Ecology Letters*, *16*(12), 1470–1479. doi:10.1111/ele.12192
- 526 Kearney, Michael R., Isaac, A. P., & Porter, W. P. (2014). microclim: Global estimates of
527 hourly microclimate based on long-term monthly climate averages. *Scientific Data*, *1*,
528 140006. doi:doi: 10.1038/sdata.2014.6
- 529 Kearney, Michael R., & Porter, W. P. (2017). NicheMapR - an R package for biophysical
530 modelling: the microclimate model. *Ecography*, *40*(5), 664–674.
531 doi:10.1111/ecog.02360
- 532 Kearney, Michael R., & Porter, W. P. (2019). NicheMapR - an R package for biophysical
533 modelling: the ectotherm and Dynamic Energy Budget models. *Ecography*, *42*, 1–12.
534 doi:10.1111/ecog.04680
- 535 Kearney, Michael R., Shine, R., & Porter, W. P. (2009). The potential for behavioral
536 thermoregulation to buffer ‘cold-blooded’ animals against climate warming.
537 *Proceedings of the National Academy of Sciences*, *106*(10), 3835–3840.

- 538 doi:<https://doi.org/10.1073/pnas.0808913106>
- 539 Kearney, Michael Ray. (2020a). Data for tests of the NicheMapR transient heat budget
540 modelling code [Data set]. Zenodo. doi:10.5281/zenodo.4146954
- 541 Kearney, Michael Ray. (2020b). *mrke/NicheMapR: NicheMapR v3.0.0*. Zenodo.
542 doi:10.5281/zenodo.4146966
- 543 King, D. (1980). The thermal biology of free-living Sand Goannas (*Varanus gouldi*) in
544 southern Australia. *Copeia*, 1980(4), 755–767.
- 545 McNab, B. K. (1963). Bioenergetics and the Determination of Home Range Size. *The*
546 *American Naturalist*, 97(894), 133–140. doi:10.1086/282264
- 547 Muth, A. (1977). Thermoregulatory Postures and Orientation to the Sun: A Mechanistic
548 Evaluation for the Zebra-Tailed Lizard, *Callisaurus draconoides*. *Copeia*, 1977(4),
549 710–720. doi:10.2307/1443171
- 550 Norris, K. S. (1967). Color adaptation in desert reptiles and its thermal relationships. In W.
551 W. Milstead (Ed.), *Lizard Ecology, A Symposium* (pp. 162–229). Columbia, Mo:
552 Univ. Mo. Press.
- 553 Pianka, E. R. (1971). Ecology of the Agamid Lizard *Amphibolurus isolepis* in Western
554 Australia. *Copeia*, 1971(3), 527. doi:10.2307/1442450
- 555 Pinsky, M. L., Eikeset, A. M., McCauley, D. J., Payne, J. L., & Sunday, J. M. (2019). Greater
556 vulnerability to warming of marine versus terrestrial ectotherms. *Nature*, 569(7754),
557 108. doi:10.1038/s41586-019-1132-4
- 558 Porter, W. P., Mitchell, J. W., Beckman, W. A., & DeWitt, C. B. (1973). Behavioral
559 implications of mechanistic ecology - Thermal and behavioral modeling of desert
560 ectotherms and their microenvironment. *Oecologia*, 13, 1–54.
- 561 Rubalcaba, J. G., Gouveia, S. F., & Olalla-Tárraga, M. A. (2019). A mechanistic model to
562 scale up biophysical processes into geographical size gradients in ectotherms. *Global*
563 *Ecology and Biogeography*, 0(0). doi:10.1111/geb.12893
- 564 Schoener, T. W. (1968). Sizes of Feeding Territories among Birds. *Ecology*, 49(1), 123–141.
565 doi:10.2307/1933567
- 566 Sears, M. W., & Angilletta, M. J. (2015). Costs and Benefits of Thermoregulation Revisited:
567 Both the Heterogeneity and Spatial Structure of Temperature Drive Energetic Costs.
568 *The American Naturalist*, 185(4), E94–E102. doi:10.1086/680008
- 569 Sears, M. W., Angilletta, M. J., Schuler, M. S., Borchert, J., Dilliplane, K. F., Stegman, M.,
570 ... Mitchell, W. A. (2016). Configuration of the thermal landscape determines
571 thermoregulatory performance of ectotherms. *Proceedings of the National Academy*

- 572 *of Sciences*, 113(38), 10595–10600. doi:10.1073/pnas.1604824113
- 573 Seebacher, F., & Shine, R. (2004). Evaluating thermoregulation in reptiles: the fallacy of the
574 inappropriately applied method. *Physiological and Biochemical Zoology*, 77, 688–
575 695.
- 576 Sinervo, B., Mendez-de-la-Cruz, F., Miles, D. B., Heulin, B., Bastiaans, E., Villagran-Santa
577 Cruz, M., ... Sites, J. W., Jr. (2010). Erosion of Lizard Diversity by Climate Change
578 and Altered Thermal Niches. *Science*, 328(5980), 894–899.
579 doi:10.1126/science.1184695
- 580 Soetaert, K., Petzoldt, T., & Setzer, R. W. (2010). Solving Differential Equations in R:
581 Package deSolve. *Journal of Statistical Software*, 33(9), 1–25.
- 582 Spotila, J. R., Soule, O. H., & Gates, D. M. (1972). The Biophysical Ecology of the Alligator:
583 Heat Energy Budgets and Climate Spaces. *Ecology*, 53(6), 1094–1102.
584 doi:10.2307/1935421
- 585 Stevenson, R. D. (1985). Body size and limits to the daily range of body temperature in
586 terrestrial ectotherms. *The American Naturalist*, 125(1), 102–177.
- 587 Sunday, J. M., Bates, A. E., Kearney, M. R., Colwell, R. K., Dulvy, N. K., Longino, J. T., &
588 Huey, R. B. (2014). Thermal-safety margins and the necessity of thermoregulatory
589 behavior across latitude and elevation. *Proceedings of the National Academy of
590 Sciences*, 111(15), 5610–5615. doi:10.1073/pnas.1316145111
- 591 Tinkle, D. W. (1967). The life and demography of the side-blotched lizard, *Uta stansburiana*.
592 *Univ. Mich. Mus. Zool. Misc. Publ.*, 132, 21–182.
- 593 Tracy, C. R., & Christian, K. A. (1986). Ecological relations among space, time, and thermal
594 niche axes. *Ecology*, 67(3), 609–615.
- 595 van Berkum, F. H., Huey, R. B., & Adams, B. A. (1986). Physiological consequences of
596 thermoregulation in a tropical lizard (*Ameiva festiva*). *Physiological Zoology*, 59(4),
597 464–47.
- 598 Vasseur, D. A., DeLong, J. P., Gilbert, B., Greig, H. S., Harley, C. D. G., McCann, K. S., ...
599 O'Connor, M. I. (2014). Increased temperature variation poses a greater risk to
600 species than climate warming. *Proceedings of the Royal Society B: Biological
601 Sciences*, 281(1779). doi:10.1098/rspb.2013.2612
- 602 Willmer, P. G., & Unwin, D. M. (1981). Field analyses of insect heat budgets: Reflectance,
603 size and heating rates. *Oecologia*, 50(2), 250–255. doi:10.1007/BF00348047
- 604
- 605

606 FIGURES

607

608 **Figure 1.** Conceptual diagram of how body size (black filled circles) alters microclimates in
609 sun, with each animal's boundary layer (white) proportional to its body mass. (a) A
610 "Newtonian"-only perspective assumes that small and large individuals experience identical
611 air temperatures (grey), wind speeds (blue arrows), and radiation loads, as might be the case
612 if they were suspended in air at midday. (b) A "Geigerian" perspective assumes additionally
613 that the larger animal experiences relatively cooler air temperatures as well as higher wind
614 speeds, which reduce the thickness of its boundary layer. Thus, a large diurnal animal on the
615 ground experiences a cooler and more convective environment at midday than does a small
616 diurnal animal on the ground.

617

618 **Figure 2.** Computed heating rates of 10-g and 1000-g ellipsoid bodies under fixed conditions.

619 A) A 'Newtonian' perspective with both the small and large objects positioned at 7.5 cm
620 above ground (the natural height of the large ectotherm) with wind speed 1.36 m s^{-1} and air
621 temperature $34.2 \text{ }^\circ\text{C}$. The small ectotherm heats relatively quickly but has a lower steady-
622 state T_b than does the large ectotherm, as expected due to boundary layer effects. B) A
623 'Geigerian' perspective has the small and large ectotherms positioned at their natural height
624 (1 vs. 7.5 cm, respectively). Here the small ectotherm, now experiencing a wind speed of
625 0.57 m s^{-1} and air temperature of $38.4 \text{ }^\circ\text{C}$, still heats quickly but has the higher steady-state
626 T_b .

627

628 **Figure 3.** Body temperature trajectories of thermoregulating 10 g (dragon) and 1000 g
629 (goanna) lizards experiencing microclimates at either 1 cm or 7.5 cm above the ground on an
630 average spring (September) or summer (January) day in central Australia.

631

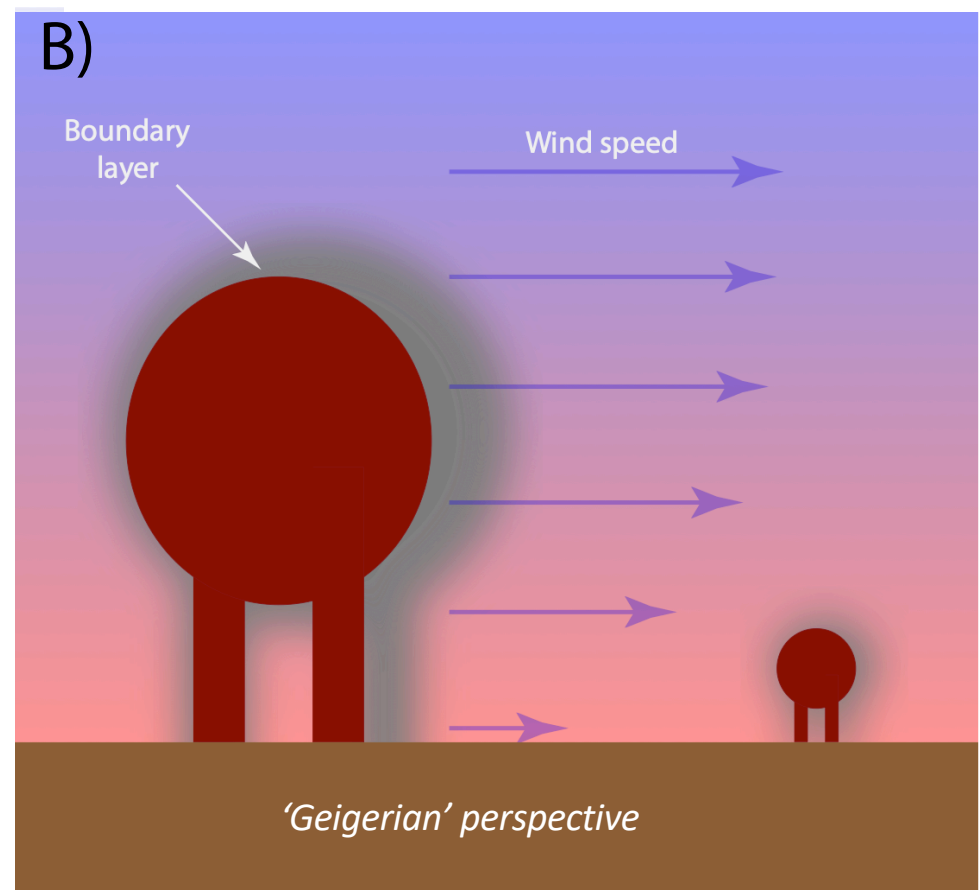
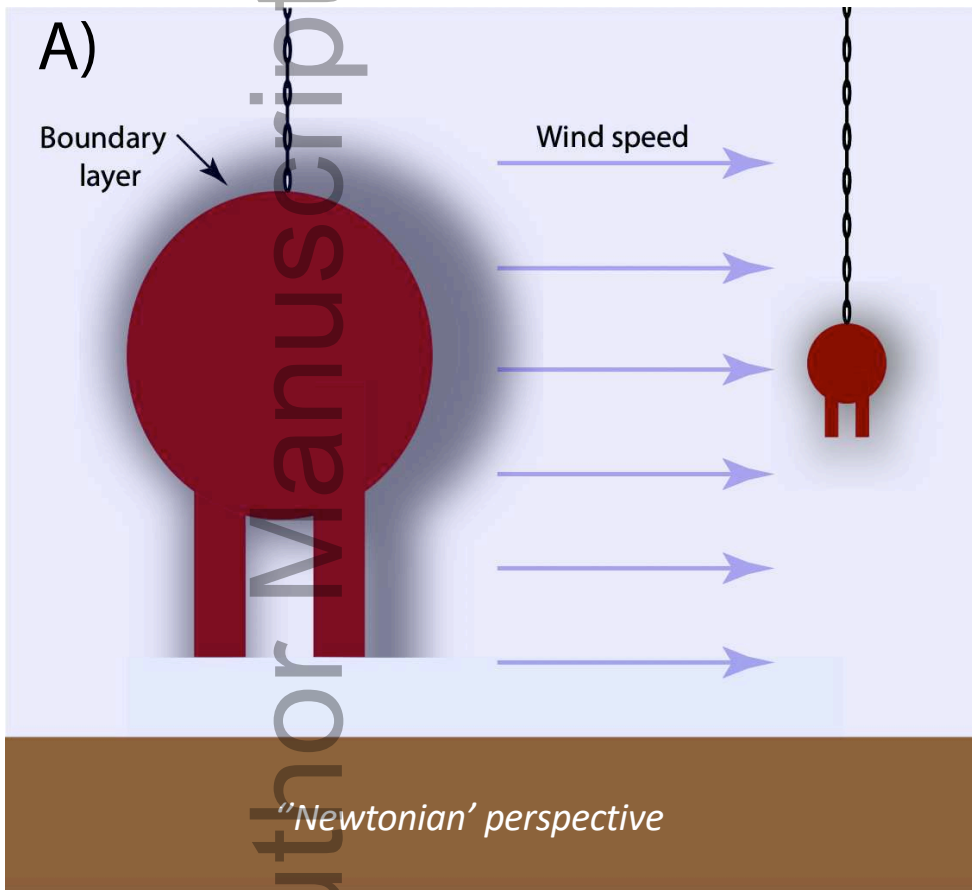
632 **Figure 4** Summary of ecological consequences of thermoregulating for a 10 g (dragon, small
633 dots, dashed line) and 1000 g (goanna, large dots, solid line) lizards experiencing
634 microclimates at either 1 cm or 7.5 cm above the ground on an average spring (September,
635 blue) or summer (January, red) day in central Australia.

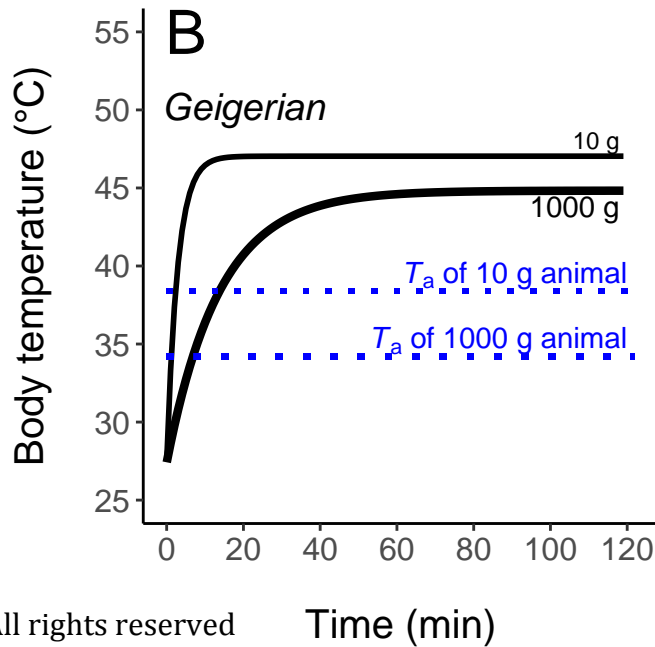
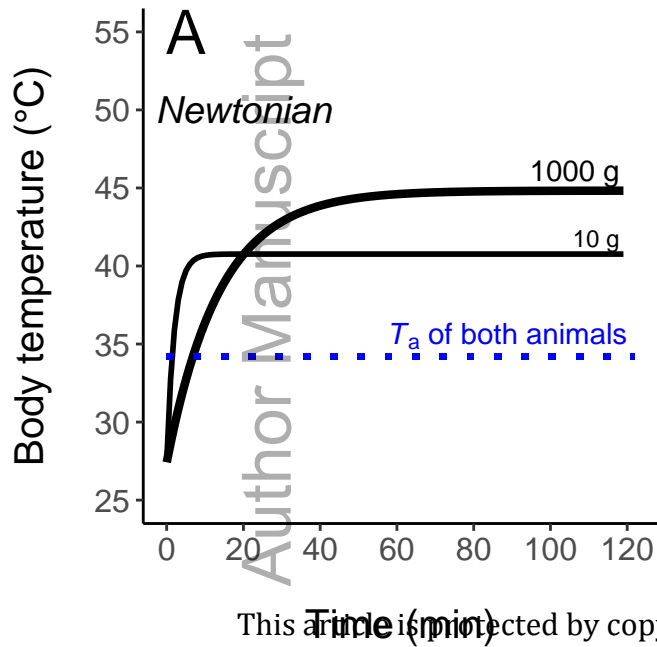
636

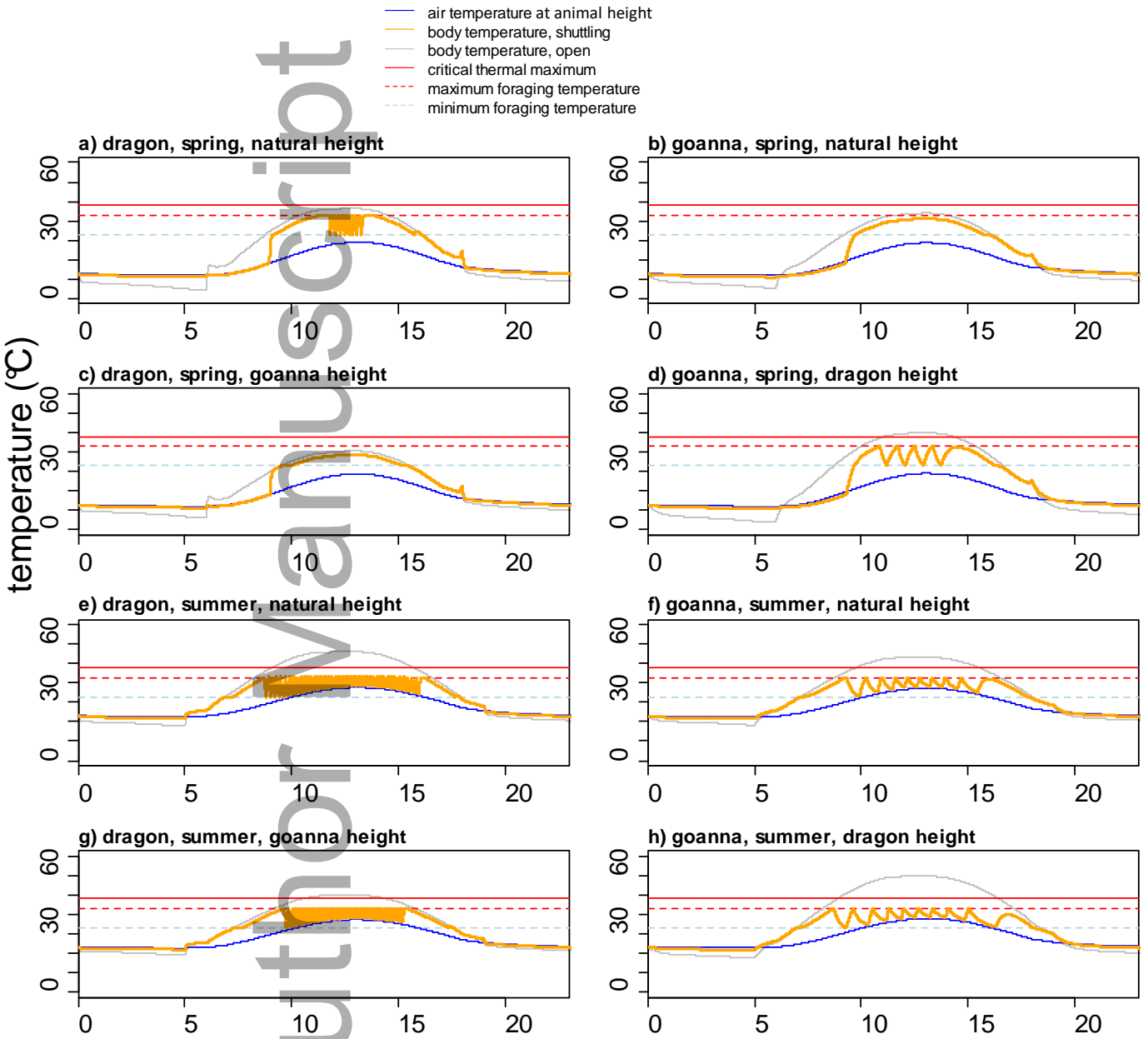
637 **Figure 5.** Maximum daily foraging radii from randomly arrayed patches of shade
638 thermoregulating 10 g (dragon) and 1000 g (goanna) lizards experiencing microclimates at

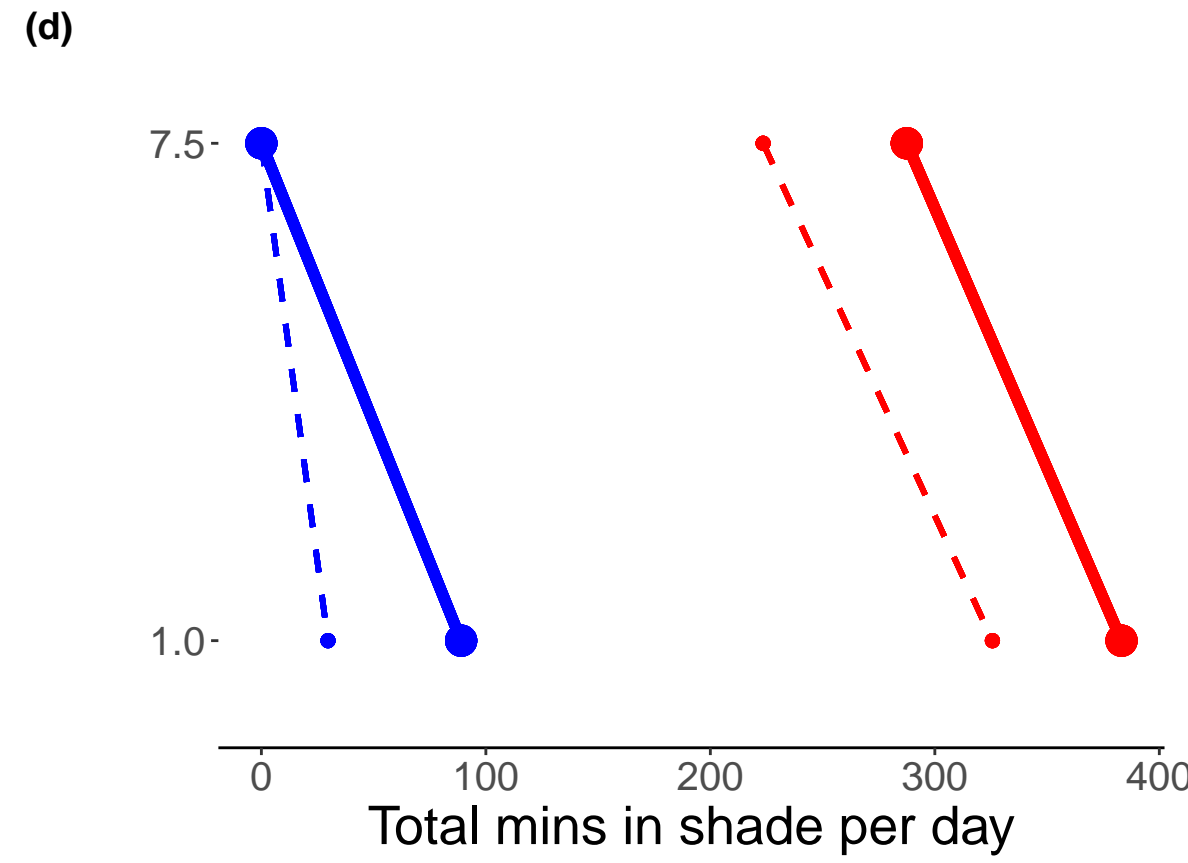
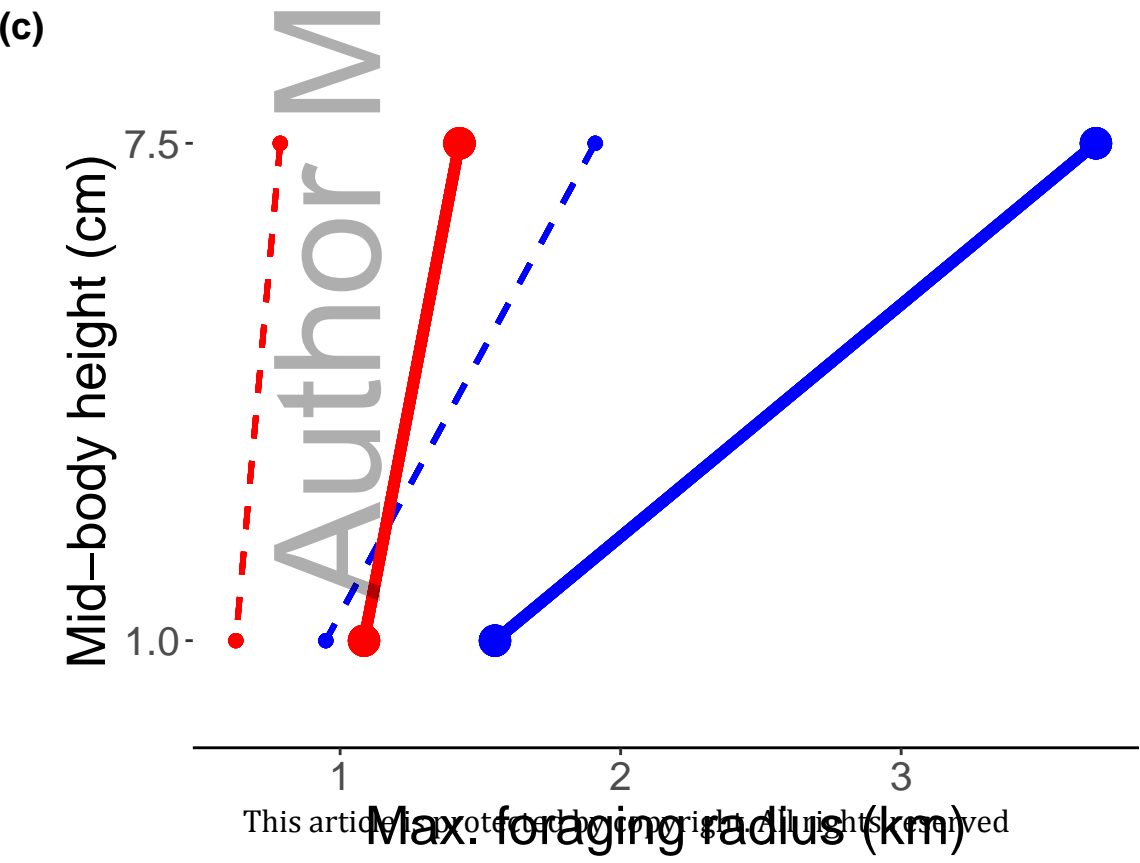
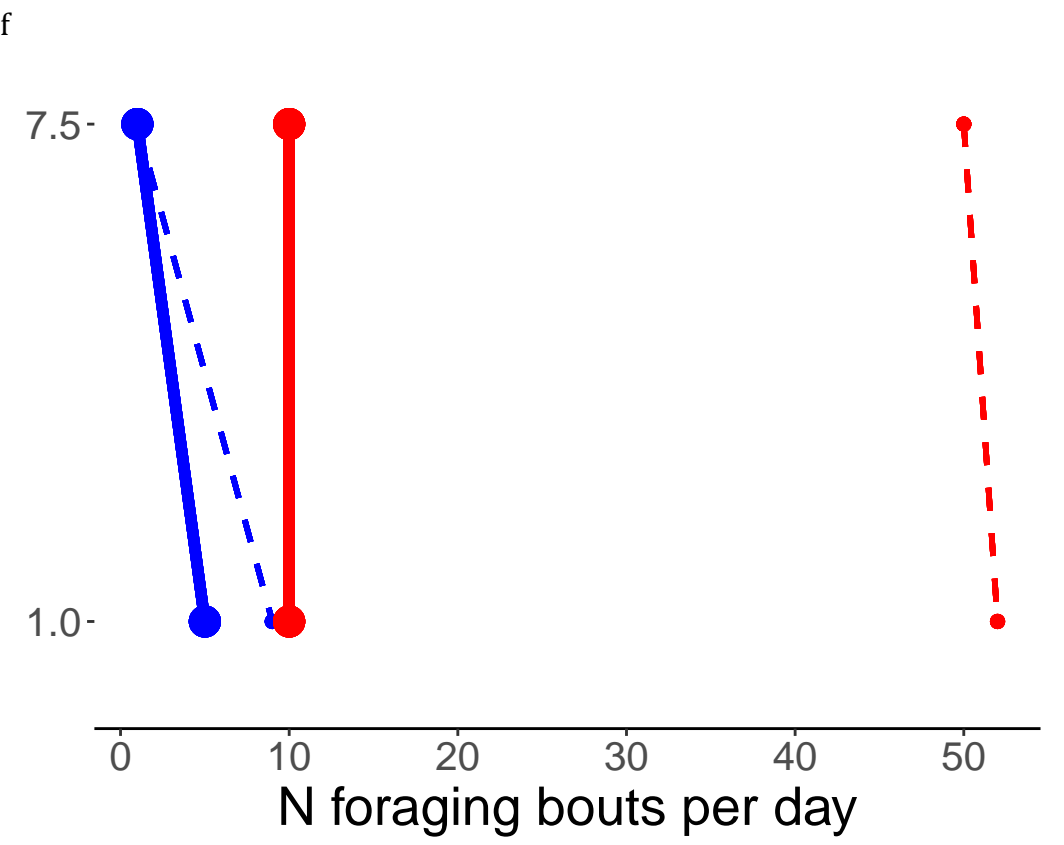
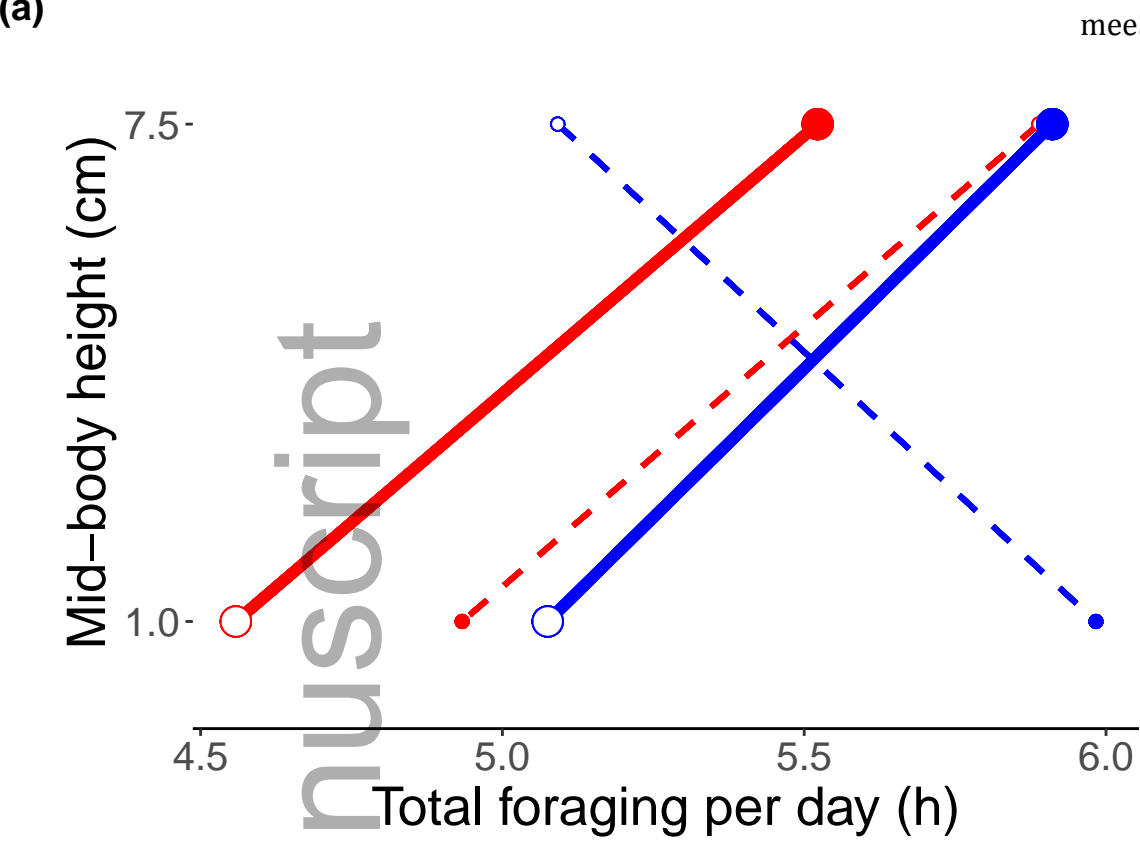
639 either 1 cm or 7.5 cm above the ground on an average spring (September) or summer
640 (January) day in central Australia.

Author Manuscript

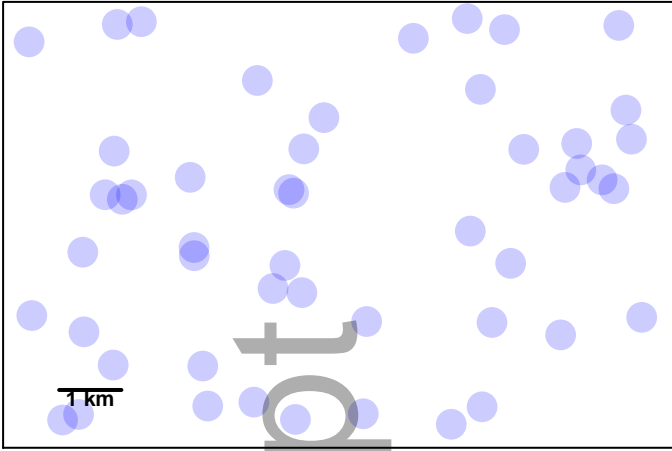




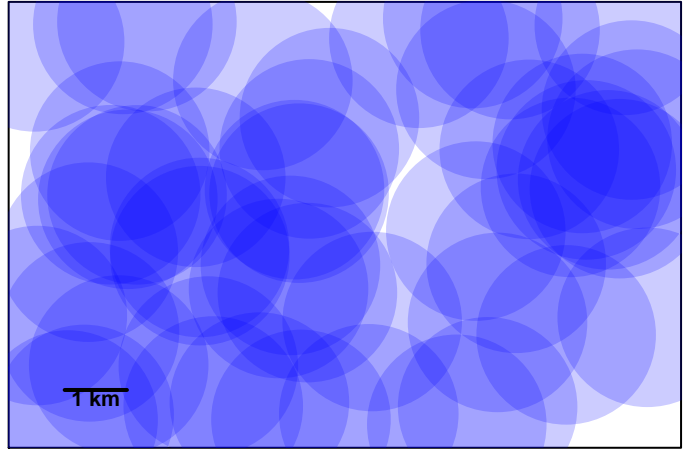




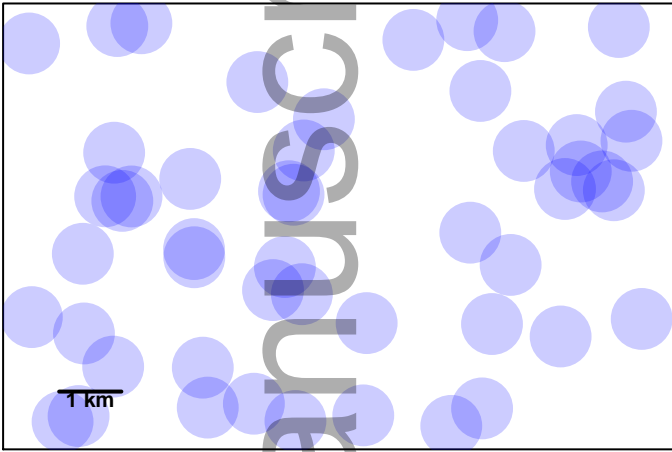
a) dragon, spring, natural height



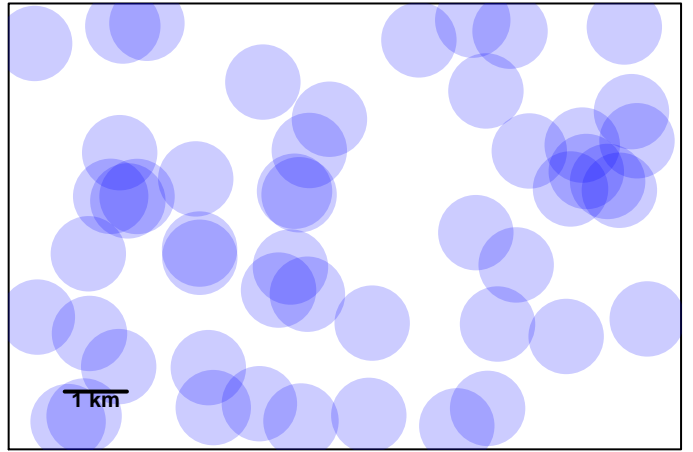
b) goanna, spring, natural height



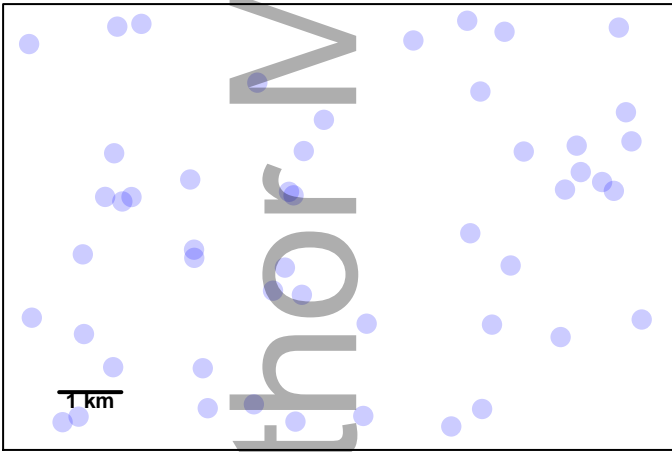
c) dragon, spring, goanna height



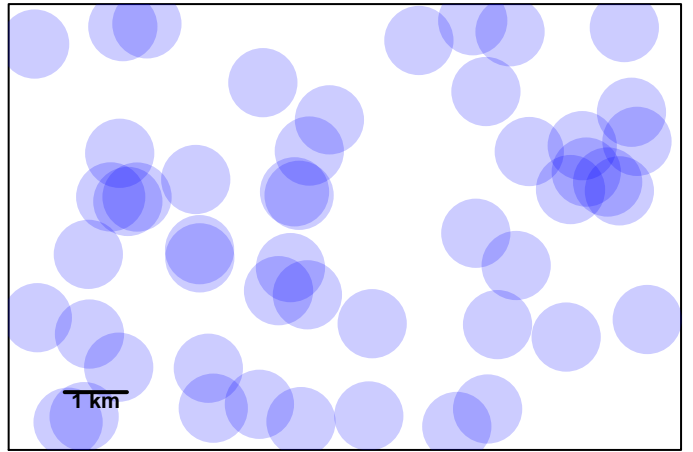
d) goanna, spring, dragon height



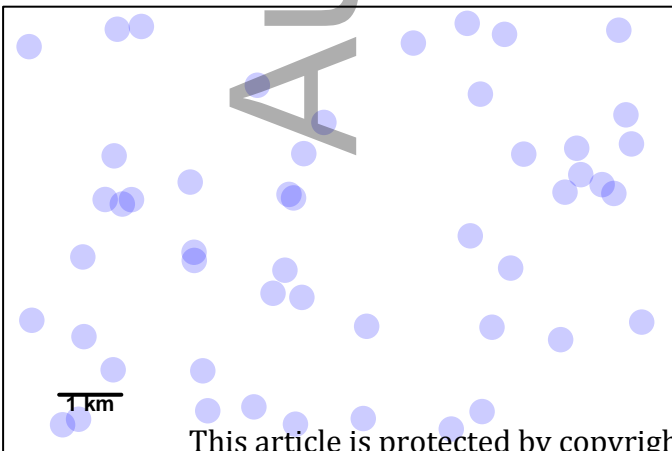
e) dragon, summer, natural height



f) goanna, summer, natural height



g) dragon, summer, goanna height



h) goanna, summer, dragon height

